Colloid Polym Sci 279:823–827 (2001)

SHORT COMMUNICATION

W. H. Jang
J. W. Kim
H. J. Choi
M. S. Jhon

Synthesis and electrorheology of camphorsulfonic acid doped polyaniline suspensions

Received: 31 August 2000
Accepted: 6 April 2001

W. H. Jang · J. W. Kim · H. J. Choi (✉)
Department of Polymer Science
and Engineering, Inha University
Inchon, 402-751, Korea
e-mail: hjchoi@inha.ac.kr

M. S. Jhon
Department of Chemical Engineering
Carnegie Mellon University
Pittsburgh, PA 15213, USA

Abstract Semiconducting camphorsulfonic acid doped polyaniline (PANI–CSA) particles were synthesized by chemical oxidation polymerization, and their chemical structure and particle size were examined via Fourier transform IR spectroscopy and scanning electron microscopy, respectively. Electrorheological (ER) fluids were prepared by dispersing the PANI–CSA particles in silicone oil, and their steady-shear rheological properties under electric fields were investigated using a rotational rheometer with a high-voltage generator. The PANI–CSA synthesized in this study possesses typical ER behavior:shear stress increases with increasing electric field strengths.

Key words Camphorsulfonic acid · Polyaniline · Chemical oxidation polymerization · Electrorheological fluid · Suspension

Introduction

Micropolarizable, nonaqueous colloidal suspensions whose rheological properties change abruptly under external electric field strengths on the order of a few kilovolts per nanometer are commonly known as electrorheological (ER) fluids, and their rheology at low-to-moderate volume fractions is known to be governed by the aggregation of particles into chainlike or columnlike structures [1]. Since their discovery, an enormous number of studies have been carried out to understand the underlying physics of ER responses and thereby to correlate the ER performance with the material properties of ER fluids. Electric-field-induced particle interaction arising from particle polarization is commonly believed to be responsible for ER behavior [2, 3].

ER fluids become highly viscous, rubberlike, or even solid, depending on the applied electric field and shear stress. ER fluid response is much faster than that in conventional mechanical systems and offers a great potential for high-technology applications, such as clutches, brakes, shock absorbers, engine mounts, valves, flow pumps, and other variable control and servo devices [4].

The dispersed phases of polarizable particle in an insulating oil play a very important role in ER phenomena. For the dispersed phase, ER systems not only use inorganic materials, such as zeolite [5] and lead zirconate titanate [6], but also polymeric particles have been adopted to solve wet-base ER fluid problems [7], such as thermal breaking and particle settling. Examples of polymeric systems include poly(acene quinone) radicals [8], copolystyrene particles with polyaniline (PANI) coating [9], PANI [10–13] and its derivatives [14,15], copolypyrrole [16], poly(aniline-*co*-*o*-ethoxyaniline) [17], poly(*p*-phenylene) [18, 19], polyphenylenediamine [20], phosphate cellulose [21, 22] and N-substituted copolyaniline [23].

Many PANI derivatives based upon modification of oxidation state, dopant, and polymerization conditions have been reported [24], since PANI has advantages over other polymer particles as a polarizable particle for ER fluids, such as density, conducting control, and thermal and environmental stability. PANI is also easy to polymerize by oxidation polymerization at relatively low temperatures and can be doped from a conducting to an insulating state using simple protonic acids. This allows a change in the particle dielectric constant and conductivity while keeping all other particle properties and suspension characteristics the same. Owing to the previously mentioned advantages, PANI has been extensively investigated as a conducting polymer [25] with various dopants.

The functional anionic group of the doping acid (e.g., aromatic or camphorsulfonic acid, CSA) is known to play an important role in improving the processability of the conductive PANI [26]. In contrast to other PANIs, the PANI–CSA system exhibits a temperature range where the electrical conductivity shows metallic-like behavior, i.e., it decreases with increasing temperature [27]. PANI–CSA exhibits very interesting processing and electrical transport properties. Cao et al. [26] reported that CSA-doped PANI is soluble in common organic solvents, such as *m*-cresol, and its electrical conductivity is much higher than that of PANI doped with inorganic acid. Recently, Rethi et al. [28] synthesized conducting PANI in a water-soluble form by an in situ method, using surfactants with strong acid functionalities as protonating agents. In addition, polyaniline-Na^+-montmorillonite nanocomposite particles were synthesized using emulsion intercalation, and their ER characteristics [29] and direct current conductivity [30, 31] were reported.

In this article we report the synthesis and investigation of CSA-doped PANI as anhydrous particles for high-performance, dry-base ER systems.

Experimental

The PANI–CSA was synthesized using an aqueous solution of CSA (Aldrich, USA), ammonium peroxysulfate [$(NH_4)_2S_2O_8$, oxidant or initiator] (Daejung, Korea), and aniline monomer (Junsei, Japan) through chemical oxidation polymerization following the method suggested by Österholm et al. [32]. The molecular structure of CSA is as follows:

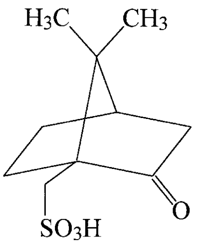

Initially, a solution composed of 23.7 g (0.25 mol) aniline, 87 g (0.375 mol) CSA, and 1.250l distilled water was prepared in a 2-l reactor. The polymerization was then initiated by the addition of 23.4 g (0.1 mol) ammonium peroxysulfate dissolved in 100 ml distilled water, which was slowly introduced to a well-stirred reactor over a period of 30 min in order to avoid overheating the reaction mixture. The polymerization temperature was maintained at 0 °C for the reaction time of 24 h. Vigorous stirring was applied to reduce temperature gradients during the reaction. The CSA-doped PANI was obtained as a dark-green (emeraldine) precipitate from the reaction system.

To make the semiconducting particles suitable for an ER fluid, we depoped the PANI particles (pH 1.2) by increasing the pH of the aqueous medium to pH 10 using a NaOH solution. The PANI–CSA synthesized was then washed using distilled water and acetone to remove the initiator, the unreacted monomer, and any oligomer. The products were finally put into a vacuum oven for 2 days of drying. The particle size of the polymers was adjusted using a mechanical mixer and a 38-μm sieve.

Characterization of the chemical structure of the PANI–CSA synthesized was conducted with a Fourier transform (FT) IR spectrometer. The shape and size distributions of the particles were determined by scanning electron microscopy (SEM). The ER fluids were then prepared by dispersing the PANI–CSA particles in silicone oil which had been dehydrated in a vacuum drying oven and stored over molecular sieves prior to use. The kinematic viscosity of the silicone oil (Lot 811664, Shinetsu, Japan) was 50 cS and the density was 0.956 g/ml at 25 °C. In this study, the particle concentration was fixed at 15 wt%.

ER characterizations were carried out using a rotational rheometer (Physica, MC120, Germany) with a Couette geometry and a high-voltage generator. To start a run, the ER fluid was placed in the gap between the stationary outer measuring cup and rotating measuring bob and a direct current voltage was applied to the cup. The probe of high-voltage generator (HVG 5000) was connected to the cup in the rheometer. The bob was the earthed to the ground. An electric field was applied to the gap between the cup and bob, and the field remained applied during the rheological measurement. The HVG 5000 could supply a direct current voltage up to 5 kV/mm within $\pm 10\ \mu$A of electric current. The flow resistance produced by the suspension was measured as a torque on the drive shaft. The electric field was applied for 3 min to obtain equilibrium chainlike or columnar structures before applying shear [5]. To get reproducible data, the ER fluid was redispersed before each experiment, and measurements were carried out at least two times. The measurement data was then obtained via controlled shear rate (CSR) and controlled shear stress (CSS) modes.

Results and discussion

The chemical structure of the PANI synthesized was identified using FT-IR analysis. The FT-IR spectra of the emeraldine base PANI and PANI–CSA polymers, determined using KBr pellets, are shown in Fig. 1.

The peaks at 1,591 and 1,497 cm^{-1} originate from aromatic C–C stretching vibrations, whereas those at 1,307 and 1,167 cm^{-1} are due to aromatic amine stretching. The peak at 832 cm^{-1} comes from the out-of-plane hydrogen deformation of aromatic rings in PANI unit sequences. Except for the characteristic peaks of the CSA that appear at 1,381 and 697 cm^{-1}, the FT-IR spectrum shows that the PANI–CSA synthesized for this study is similar to that of an emeraldine base.

The shape and the size of the PANI–CSA particles determined by SEM are shown in Fig. 2. The shape of the particles is very irregular, and the size range of the particles is approximately 1–10 μm. The irregular and laminar structure seems to arise from the rigid molecular structure of the PANI.

The shear stress versus shear rate response obtained from the CSR test for a 15 wt% suspension of the PANI–CSA at different electric field strengths is shown in Fig. 3. The shear stress increases with shear rate in an applied electric field, and it also increases over the entire shear rate range with increasing electric field strengths. Furthermore, the shear stress exhibits a plateau region over a broad range of shear rate. Figure 3 shows the result of structural changes of the ER fluid due to the shear rate. The particle chains, which are formed by the electric field, are disrupted by the shear rate. When the shear rate is high enough, the particle chains break and do not have enough time to realign themselves with the electric field.

In the low shear rate region, the shear stress developed by the applied electric field decreased as the shear rate increased up to a certain critical value, and increased afterwards. Even though the critical shear rate is not sharp, the stress of the ER fluid seems to converge to the zero-field value. The decrease in shear stress below the critical shear rate is a consequence of the destruction rate of the particle chain structures exceeding the reformation rate of the chains as the shear rate is increased [33]. The electrostatic interaction between the particles is thought to be more important than the hydrodynamic interaction below the transition point and vice versa with a further increase in shear rates

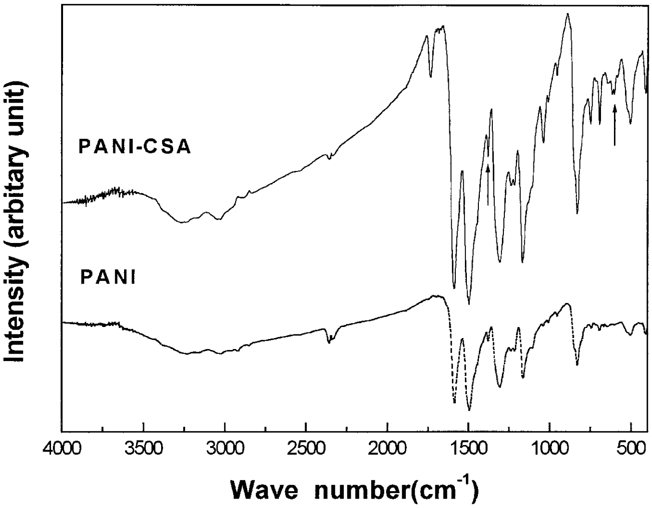

Fig. 1 Fourier transform IR spectra for polyaniline (*PANI*) and PANI– camphorsulfonic acid (*CSA*)

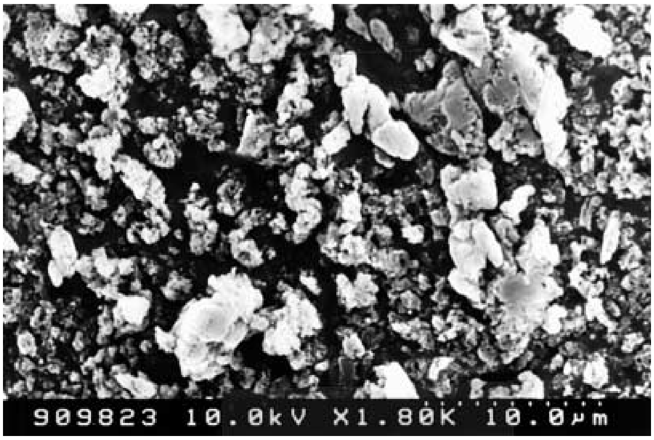

Fig. 2 Scanning electron microscopy photograph of the PANI–CSA particles

Fig. 3 Shear stress versus shear rate for a PANI–CSA electrorheological fluid at various electric field strengths (15 wt%)

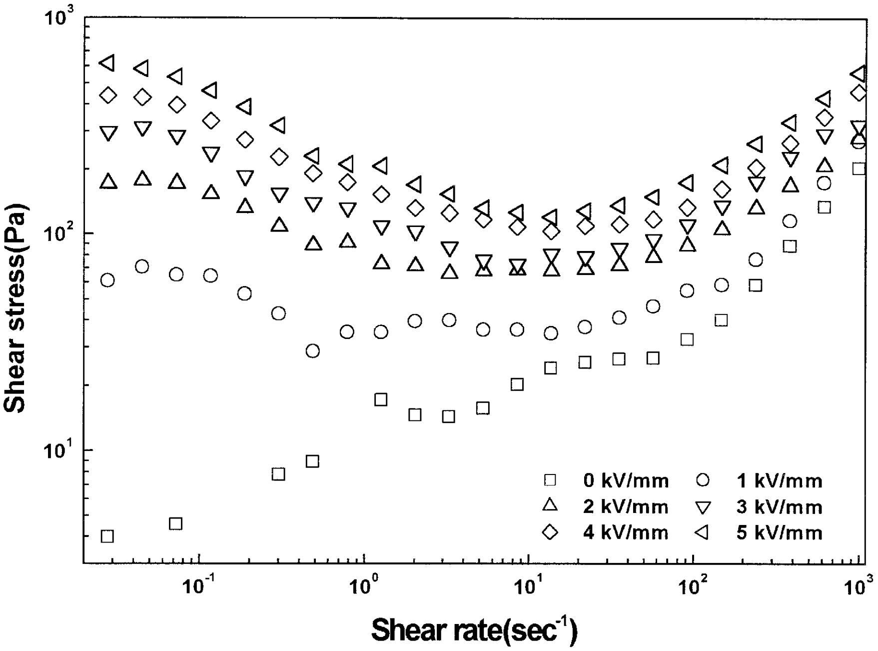

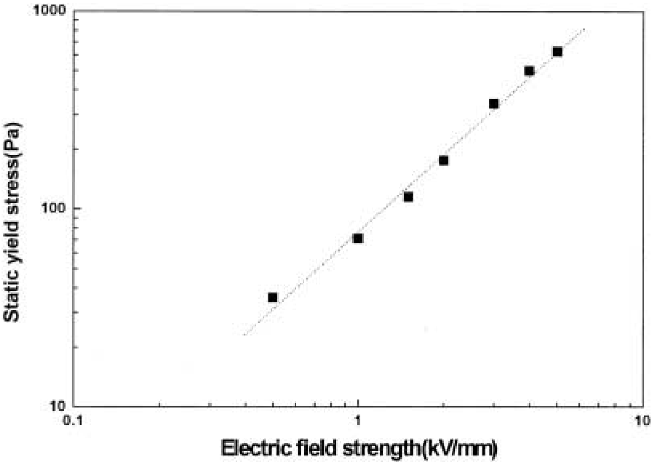

Fig. 4 Static yield stress versus electric field strength for electrorheological fluids using PANI–CSA (15 wt%)

beyond the transition point. More specifically, the decrease in shear stress below the critical shear rate can also be related to the fact that the interparticle forces are not strongly dependent on the magnitude of the local electric current flowing in the vicinity of each particle, as observed by Atten et al. [34]. This would induce an electric current decrease with increasing shear rate and reduce the interaction force between particles, showing the decrease in shear stress. A critical shear rate has also been observed for a styrene–acrylonitrile copolymer–clay nanocomposite based ER fluid [35]. Figure 3 also shows that the PANI–CSA-based fluid is electrically stable up to 5 kV/mm.

The dependence of the static yield stress on various electric field strengths for PANI–CSA obtained from the CSS mode measurements is presented in Fig. 4. The CSS mode was used to measure the static yield stress. The ER fluids is stressed by an applied mechanical torque until the particle chain structure is perfectly broken so that the shear occurs; thereby, the shear rate is observed when the flow of the ER fluid starts. The stress at this point is known as a static yield stress. Similar to many other ER fluid systems, the PANI–CSA/silicone oil ER system also possesses the property that the yield stress increases as the electric field strength increases. The conductivity of the PANI–CSA was found to be 4.4×10^{-12} S/cm. In the region of pH 10, the electrical stability of the PANI–CSA was observed to be very good. (up to 5 kV/mm) Generally, the correlation of the static yield stress (τ_y) to the electric field strength (E) at the same concentration is expressed as $\tau_y \propto E^{\alpha}$ [36, 37].

The value of α in this study was 1.34. This result differs from the theoretical prediction from the polarization model that $\alpha = 2$. This is explained by the fact that the origin of the yield stress lies in the interaction between the polarization, P, of the microspheres [6]. As a result, it is expected that the yield stress should be proportional to P^2. From linear response theory, $P \propto E$, so the yield stress is proportional to E^2. Under the applied electric field, the polarization forces increase with increasing electric field strength, which in turn increases the particle chain length, thus increasing the yield stress. When the particle concentration is too small, there are few particle chains or fibrils owing to the small polarization forces, and there is only a minute increase in the static yield stress. The occurrence of yield stress may be attributed to the surface polarization, which is determined by the electron movement within the PANI–CSA particles and electron hopping between the PANI–CSA particles under a high-voltage electric field [38]. When the electron movement within the PANI–CSA particles plays the important role in the surface polarization, the yield stress increases.

In conclusion, the chemical structure and the particle size of CSA-doped PANI were examined via FT-IR spectroscopy and SEM, respectively. ER characteristics using CSA-doped PANI as a dispersed phase in silicone oil were observed and the yield stress increased with increasing electric field strengths.

Acknowledgement This study was supported by a grant from the KOSEF through the Applied Rheology Center at Korea University, Korea.

References

1. Halsey TC, Toor W (1990) Phys Rev Lett 65:2820–2823
2. Tao R, Sun JM (1991) Phys Rev Lett 67:398–401
3. See H (2000) J Phys D Appl Phys 33:1625–1633
4. Brooks DA (1999) Int J Mod Phys B 13:2127–2134
5. Cho MS, Choi HJ, Chin IJ, Ahn WS (1999) Micropor Mesopor Mater 32:233–239
6. Wen W, Tam WY, Sheng P (1998) J Mater Sci Lett 17:419–421
7. Choi HJ, Cho MS, Kang KK, Ahn WS (2000) Micropor Mesopor Mater 39:19–24
8. Choi HJ, Cho MS, Jhon MS (1999) Int J Mod Phys B 13:1901–1907
9. Kuramoto N, Yamazaki M, Nagai K, Koyama K, Tanaka K, Yatsuzuka K, Higashiyama Y (1995) Rheol Acta 34:298–302
10. Lee JH, Cho MS, Choi HJ, Jhon MS (1999) Colloid Polym Sci 277:73–76
11. Choi HJ, Kim TW, Cho MS, Kim SG, Jhon MS (1997) Eur Polym J 33:699–703
12. Gozdalik A, Wycislik H, Plocharskii J (2000) Synth Met 109:147–150
13. Kim SG, Kim JW, Choi HJ, Suh MS, Shin MJ, Jhon MS (2000) Colloid Polym Sci 278:894–898

14. Cho MS, Kim JW, Choi HJ, Webber RM, Jhon MS (2000) Colloid Polym Sci 278:61–64
15. Trlica J, Sáha P, Quadrat O, Stejskal J (2000) Euro Polym J 36:2313–2319
16. Goodwin JW, Markham GM, Vincent B (1997) J Phys Chem B 101:1961–1967
17. Choi HJ, Kim JW, To K (1999) Synth Met 101:697–698
18. Choi HJ, Sim IS, Jhon MS (2000) J Mater Sci Lett 19:1629–1631
19. Sim IS, Kim JW, Choi HJ, Kim CA, Jhon MS (2001) Chem Mater 13:1243–1247
20. Trlica J, Sáha P, Quadradt O, Stejskal J (2000) Physica A 283:337–348
21. Kim SG, Choi HJ, Jhon MS (2001) Macromol Chem Phys 202:521–526
22. Kim SG, Kim JW, Jang WH, Choi HJ, Jhon MS (2001) Polymer 42:5005–5012
23. Cho MS, HJ Choi, K To (1998) Macromol Rapid Commun 19:271–273
24. Liao YH, Angelopoulos M, Levon K (1995) J Polym Sci Part A Polym Chem 33:2725–2729
25. Joo JS, Long SM, Pouget JP, Oh EJ, Macdiarmid AG, Epstein AJ (1998) Phys Rev B 57:9567–9580
26. Cao Y, Smith P, Heeger AJ (1992) Synth Met 48:91–97
27. Holland ER, Pomlret SJ, Adams PN, Monkman AP (1996) J Phys Condens Matter 8:2991–3002
28. Rethi M, Ponrathnam S, Rajan CR (1998) Macromol Rapid Commun 19:119–122
29. Kim JW, Kim SG, Choi HJ, Jhon MS (1999) Macromol Rapid Commun 20:450–452
30. Kim BH, Jung JH, Joo J, Kim JW, Choi HJ (2000) J Korean Phys Soc 36:366–370
31. Kim BH, Jung JH, Kim JW, Choi HJ, Joo J (2001) Synth Met 117:115–118
32. Österholm J, Cao Y, Klavetter F, Smith P (1992) Polymer 35:2902–2906
33. Shih YH, Conrad H (1994) Int J Mod Phys B 8:2835–2853
34. Atten P, Boissy C, Foulc J-N (1997) J Electrostatics 40/41:3–12
35. Kim JW, Noh MH, Choi HJ, Lee DC, Jhon MS (2000) Polymer 41:1229–1231
36. Otsubo Y, Sekine M, Katayama S (1991) J Colloid Interface Sci 146:395–404
37. Block H, Kelly JP (1988) J Phys D Appl Phys 21:1661–1677
38. Xie HQ, Guan JG, Guo JS (1997) J Appl Polym Sci 64:1641–1647